This article has been accepted for publication in a future issue of this journal, but has not been fully edited. Content may change prior to final publication.

Optimal Torque Control of Synchronous Machines based on Finite Element Analysis

Hugo W. de Kock, *Member, IEEE,* Arnold J. Rix, *Member, IEEE,* and Maarten J. Kamper, *Senior Member, IEEE*

***Abstract*—Synchronous machines that are optimally designed using finite element software, and control of such machines using powerful digital signal processors, is common-place today. With field orientated control, the maximum torque per Ampere control strategy for unsaturated voltage conditions (below base speed) is well known; the field weakening strategy however, could be rather complicated. In this paper a straightforward torque control strategy for the entire speed range is proposed and demonstrated. Practical implementation of the method is very simple, since the calculations are done off-line in an automated process and are therefore removed from the load of the digital signal processor. The process relies on machine specific data from finite element analysis and therefore includes non-linear effects such as saturation and cross-coupling. Simulated and practical results for a permanent magnet- and a reluctance synchronous machine show that the torque is controlled effectively in the entire speed range using this generic method.**

***Index Terms*—Synchronous machines, Torque control, Finite Element Analysis**

I. Introduction

The focus on high efficiency and cost effective drives, for applications ranging from washing machines to electrical vehicles, has led to the adoption of certain types of synchronous machines, with control algorithms that maximize efficiency and avoid the use of expensive sensors [1], [2]. The permanent magnet synchronous machine (PMSM) is a popular choice for many applications (e.g. servo drives) since it has high efficiency, high power density and a very wide speed range. The reluctance synchronous machine (RSM) typically has a smaller speed range compared to a PMSM with a similar power rating. This could be understood by considering that additional voltage is needed to generate magnetizing flux for the RSM, where in the PMSM it is not needed due to the permanent magnets. Above base speed the availability of voltage for producing torque (not magnetizing flux) is what determines its field weakening performance. Still the RSM is a viable alternative for many applications (e.g. fans and pumps) and is attractive due to its low material cost [3], [4].

In order to achieve a cost effective, robust and reliable drive, it is a requirement to have position sensorless control, i.e. rotor position estimation in the full speed range. Those kinds of PMSMs and RSMs that exhibit high frequency saliency characteristics are advantageous since they are prime candidates for rotor position estimation at zero speed [5]–[9]. The introduction of concentrated stator windings (instead of distributed stator windings) represents another cost-saving effort, although this has some implications for the fundamental control, as well as sensorless control [10].

On the other hand, to achieve high efficiency and wide speed operation, the torque control algorithm needs to be optimized. Two main schools of thought have emerged in this regard namely direct torque control (DTC) [11]–[20] and field orientated control (FOC) [1], [21]–[30], although it is not always possible to make such clear distinction and sometimes a combination of methods or a different approach is used [31], [32].

Manuscript received February 27, 2009. Accepted for publication July 28, 2009.

H.W. de Kock is with Optimal Energy, Cape Town, South Africa. E-mail: hugodekock@gmail.com

A.J. Rix and M.J. Kamper are with the Electrical and Electronic Engineering Department at Stellenbosch University, Stellenbosch, South Africa. E-mail: rix@sun.ac.za, kamper@sun.ac.za

Nomenclature

$\vec{u}_r$	stator voltage vector in the rotating dq reference frame
α_r	stator voltage angle in the rotating dq reference frame
$\vec{i}_r$	stator current vector in the rotating dq reference frame
ϕ_r	stator current angle in the rotating dq reference frame
$\vec{\psi}_r$	stator flux linkage vector in the rotating dq reference frame
δ_r	stator flux linkage angle in the rotating dq reference frame
ω_r	electrical rotational speed
R_s	stator resistance
T_m	machine torque
p	number of pole pairs
PMSM	permanent magnet synchronous machine
IPMSM	interior permanent magnet synchronous machine
RSM	reluctance synchronous machine
2D	two dimensional
LUT	lookup table
FE	finite element
FOC	field oriented control
DTC	direct torque control
MTPA	maximum torque per Ampere
FW	field weakening

Some torque control strategies within the field oriented control (FOC) category, similar to what is presented in this paper, have been suggested [21], [25]–[27]. In [21], the torque control problem is explained very well. The q-axis current reference is given by a PI speed controller, and the d-axis current reference is calculated: a decision between maximum torque per Ampere (MTPA) or field weakening (FW) control is made based on the measured speed, and in both cases, the d-axis current reference is calculated using analytical machine equations with constant parameters. High dynamic decoupling current controllers are used to give the voltage reference. A voltage reference compensation function, to limit the voltage reference in a way that give preference to controlling the d-axis current, is also suggested. It has been demonstrated that this kind of control is capable of a fast dynamic response. The switch-over from MTPA to FW does not seem to be a problem, using the given decision-making trees. In [27] and [26] similar ideas are presented.

The focus of this paper is on the torque control strategy. The proposed algorithm falls into the FOC category. Maximum torque per Ampere and efficient field weakening is implemented using a set of 2D lookup tables (LUT) that directly translate the torque reference to the correct current vector reference in the synchronously rotating dq reference frame, for any given speed and DC bus voltage. This is similar to the work in [25], although in this paper the method for obtaining the 2D LUTs is explained in full detail.

In this paper, the first example where the torque control algorithm has been applied is on an interior permanent magnet synchronous machine (IPMSM) [1]. The IPMSM has concentrated stator windings and a high number of pole pairs. The application for the IPMSM is an electrical vehicle; the power rating is 10 kW. The proposed drive technology is to use in-wheel motors, also called hub-motors, for direct drive. The IPMSM has been optimally designed using 2D finite element (FE) software so that it complies with the necessary performance requirements [33].

The second example where the torque control has been applied is on a reluctance synchronous machine (RSM) [2]. The RSM has normal distributed stator windings and a low number of pole pairs. It is a small laboratory machine with only 1.5 kW power rating and is used purely for experimental work. The RSM rotor design has been optimized using the same 2D FE software as in the example above.

In section II a generic machine model is given and FE results for both IPMSM and RSM are shown. The FE results (in polar coordinates) describe machine behaviour very accurately and the limitations that the drive system impose (limited DC bus voltage, machine current limit) are clearly visible. The torque control concept is explained in section III and implementation details is given in section IV. Simulation and practical results are shown in section V.

II. Machine model

The rated conditions and related information of the IPMSM and RSM that are used as examples are given in Tables I and II. The IPMSM has 40 poles with a non-overlap concentrated stator winding and an interior permanent magnet rotor while the RSM has 4 poles with a distributed stator winding.

The FE model cross sections are shown in Fig. 1(a) and Fig. 1(b). The results from FE analysis shown in Fig. 2 describe the IPMSM and RSM in polar coordinates. The input current vector to the FE program is $\vec{i_r}$ and the electro-static solution gives $\vec{\psi_r}$. T_m is solved using (2), and $\vec{u_r}$ is solved in the steady state using (1) with ω_r as an independent variable.

$$\vec{u}_r = R_s\vec{i}_r + \frac{d\vec{\psi}_r}{dt} + j\omega_r\vec{\psi}_r \tag{1}$$

$$T_m = \frac{3p}{2} j\vec{\psi}_r \cdot \vec{i}_r \tag{2}$$

Fig. 2(a) shows the current $\vec{i_r}$ of the IPMSM with the outer circle corresponding to the rated current magnitude. Fig. 2(b) shows the corresponding flux linkage $\vec{\psi_r}$ for the IPMSM, where it can be noted that saturation occurs in the positive d-axis. Fig. 2(c) shows the torque magnitude $|T_m|$ with current angle ϕ_r for the IPMSM, i.e. the effect that current angle has on torque production for various current magnitudes. It allows one to easily identify maximum torque per ampere (MTPA) points. Filled circles indicate MTPA points with corresponding MTPA points shown on Figs. 2(a), 2(b) and 2(d).

Fig. 2(d) shows the voltage evaluated for the rated speed of the IPMSM using (1). Considering the voltage limitation imposed by the drive system, as indicated by the dotted circle, achievable operating conditions are limited to the region within the circle (the solid lines) and unachievable operating conditions outside the circle (the dotted lines), as shown in Fig. 2(d). This voltage restriction is reflected on the current, flux linkage and torque graphs as shown in Figs. 2(a), 2(b) and 2(c) respectively.

Similarly, Fig. 2(g) shows the current $\vec{i_r}$ of the RSM with the outer circle corresponding to the rated current magnitude. Fig. 2(h) shows the corresponding flux linkage $\vec{\psi_r}$ for the RSM, where saturation in both positive and negative d-axis is clearly visible. Fig. 2(i) shows the torque magnitude $|T_m|$ with current angle ϕ_r for the RSM. Filled circles indicate maximum torque per ampere (MTPA) with corresponding MTPA points shown on Figs. 2(g), 2(h) and 2(j). Fig. 2(j) shows the voltage evaluated for the rated speed of the RSM using (1). Considering the voltage limitation imposed by the drive system, as indicated by the solid-line circle, achievable operating conditions are limited to the region within the circle (the solid lines) and unachievable operating conditions outside the circle (the dotted lines), as shown in Fig. 2(j). This voltage restriction is reflected on the current, flux linkage and torque graphs as shown in Figs. 2(g), 2(h) and 2(i) respectively.

III. Suggested torque control algorithm

From FE analysis we know that the machine parameters are not constant, and in applications such as electrical vehicles where the DC bus voltage has a wide operating range, a decision for the current vector reference based only on the measured speed will not work. Any scheme that is based on parameter approximations of the non-linear functions, and that uses complicated decision trees and iteration, is not the

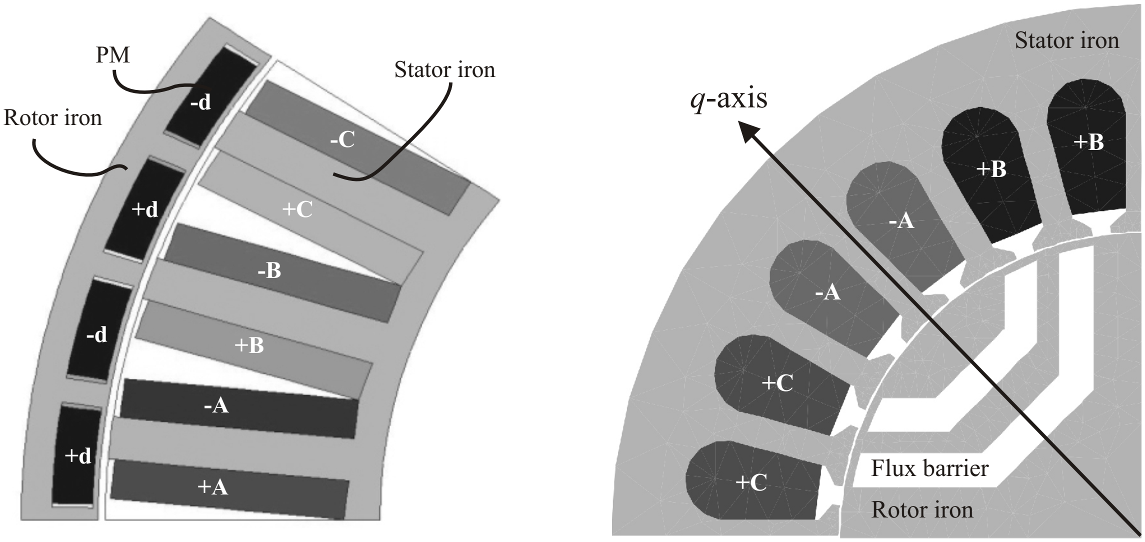

(a) IPMSM with concentrated windings.

(b) RSM with distributed windings.

Fig. 1. FE models.

TABLE I
IPMSM RATED VALUES AND RELATED INFORMATION.

Speed	300 rpm	Frequency	100 Hz
Voltage	73 V rms l-l	Voltage angle	167 °
Current	110 A rms	Current angle	117 °
Flux linkage	0.085 V.s	Flux angle	82 °
Power	10 kW	Power factor	0.64
Torque	250 N.m	DC bus	120 V
Pole pairs	20	Stator slots	30

TABLE II
RSM RATED VALUES AND RELATED INFORMATION.

Speed	1500 rpm	Frequency	50 Hz
Voltage	400 V rms l-l	Voltage angle	110 °
Current	3.5 A rms	Current angle	60 °
Flux linkage	1 V.s	Flux angle	20 °
Power	1.5 kW	Power factor	0.63
Torque	10 N.m	DC bus	625 V
Pole pairs	2	Stator slots	24

simplest and most elegant solution. For industry acceptance, a scheme that is easy to implement, is always an advantage.

The suggested torque control algorithm is illustrated by Fig. 3. Current vector control in the synchronously rotating reference frame using space vector PWM is used. In Fig. 3, the block C(s) is a PI controller (with anti-windup and speed-voltage decoupling) and W(s) is a speed observer [34]. The flux linkage magnitude restriction is calculated using the measured speed (electrical rad/sec) and the measured DC bus voltage. The correct current vector reference for the requested torque, under the flux linkage magnitude restriction, is then obtained from a set of two-dimensional (2D) lookup tables, i.e. one 2D LUT is used for the d-axis current reference as a function of both torque reference and maximum allowable flux linkage magnitude $i_d^*(T_m^*, |\psi_r|_{MAX})$ and one 2D LUT is used for the q-axis current reference as a function of both torque reference and maximum allowable flux linkage magnitude $i_q^*(T_m^*, |\psi_r|_{MAX})$. Two dimensional interpolation is used so the lookup table size can be reduced.

In this method, there is a direct translation from the torque reference and flux linkage magnitude restriction to the current vector reference. There are no complicated equations, approximation or any decision making tables, plus the method may work at any speed and any DC bus voltage. Therefore, the calculation effort has been removed from the load of the DSP and is rather performed off-line in an automated process. Practical implementation only requires the tables to be stored in memory and possibly a procedure for 2D interpolation.

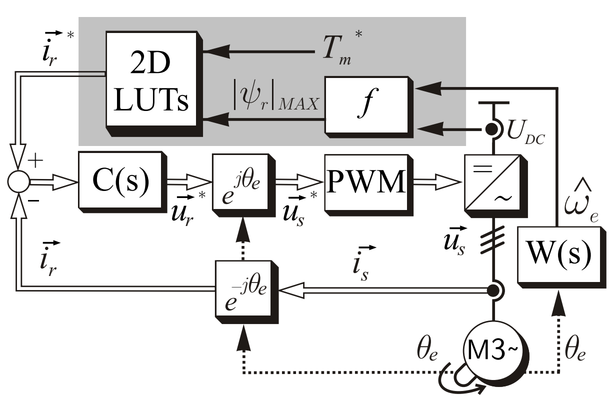

Fig. 3. Torque control block diagram.

IV. Lookup table creation

Results from FE analysis are used directly by a program that creates 2D lookup tables: the torque reference and maximum flux linkage are inputs, and the i_d and i_q references are outputs. In the program, a series of constraints are expressed as contour lines on the dq current plane and decision making logic is used to find the correct current references. The MTPA contour is used as the line that represents the optimal solution. The torque reference contour and maximum flux linkage contour, as well as the maximum current contour (and maximum negative i_d in the case of the IPMSM) represent the constraints. The program flow diagram is shown in Fig. 4.

This program for creating the 2D LUTs can execute within minutes. The FE results needed by the program (the current to flux linkage mapping) could also be obtained within a short amount of time. Concerning the control program, the table size for the 2D LUTs can be fairly small if 2D interpolation is used. A lookup operation is much faster than iterative decision making logic during execution. The method is exact, because it uses the FE results directly: there is not even an attempt to linearize or find approximation functions. The LUTs that were used inside the control programs are illustrated by Figs. 2(e) and 2(f) for the IPMSM, and in Figs. 2(k) and 2(l) for the RSM.

V. Simulation and practical results

The torque control algorithm was simulated for both IPMSM and RSM, using machine models that include sets of 2D tables from FE analysis for the mapping between current and flux linkages, i.e. the effect of saturation and mutual coupling is modelled. The effect of non-sinusoidal flux linkage distribution during rotation, i.e. flux pulsation, and torque ripple, as well as iron-losses are neglected.

As a first step towards practical verification on the IPMSM, the torque as a function of current angle for various current magnitudes (0.33, 0.66 and 1.0 per unit) has been measured with a torque sensor and compared with the FE results, as shown in Fig. 5(a) [1]. This confirms that the actual IPMSM performs as predicted by the FE model. Steady state practical measurements have been performed to test the control strategy and to compare it with the simulation results, as shown in Fig. 5(b). The results show that this open loop torque control strategy is effective in the steady state. Moreover, the iron loss has a negligible effect and may be omitted in the current vector reference selection, since the simulated and practical measurements correlate well although the iron loss is neglected in the simulation, and it must be present in the practical measurement.

The torque control algorithm was also implemented for the RSM using the same methodology, but on a different system [2]. A dynamic test was performed whereby a torque reference reversal is applied under no load conditions, i.e. first a positive torque reference of 9 Nm is given (rated toque) and the machine is allowed to speed up and go into flux weakening; then a negative torque reference of -9 Nm is given and the machine is allowed to reverse its speed. The simulation result is shown in Fig. 6(a) and the practical result is shown in Fig. 6(b). The simulation and practical tests were performed using a rapid prototyping system. Important to note is that equal performance in both directions is obtained. This test shows that the torque control algorithm also performs well during transient conditions.

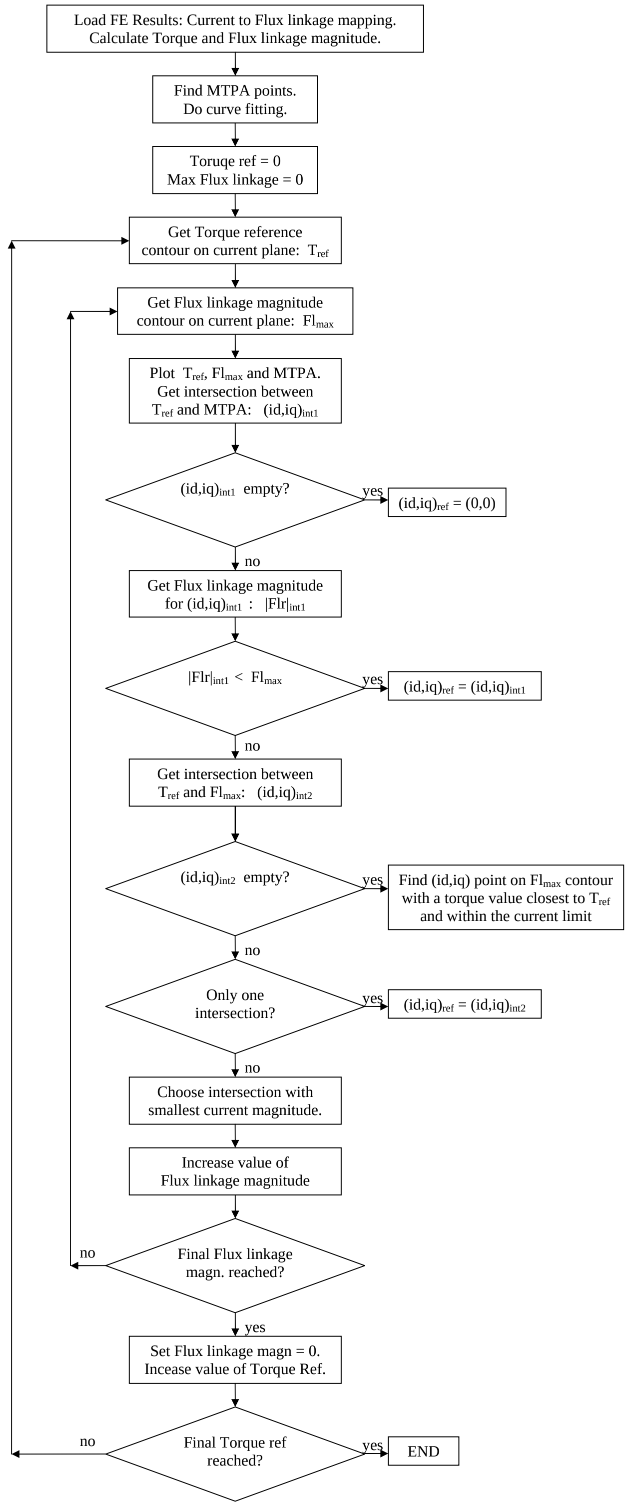

Fig. 4. 2D LUTs setup program.

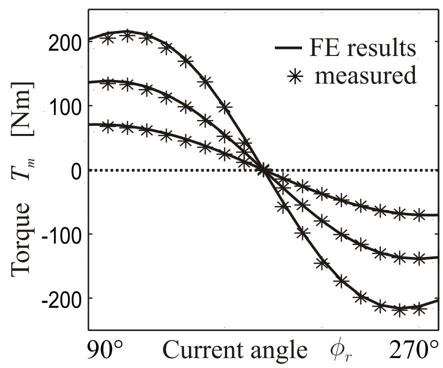

(a) T_m vs. ϕ_r, for i_r = 0.33, 0.66 and 1.0 p.u.

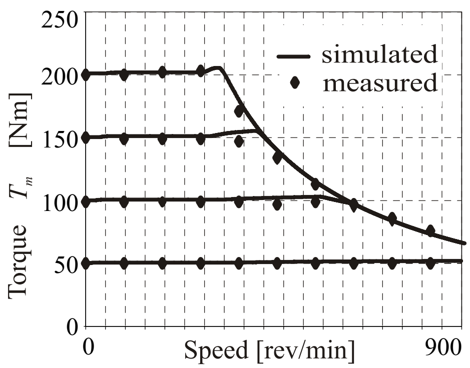

(b) T_m vs. speed

Fig. 5. Practical and simulation results for IPMSM.

VI. Conclusion

A generic torque control algorithm for synchronous machine drives that works in the entire speed range and for variable DC bus voltage is proposed and demonstrated. An IPMSM with concentrated stator windings and a RSM with distributed stator windings were used as examples. The suggested torque control algorithm is based on a set of 2D LUTs that are generated directly from FE results and the method to obtain these tables is fully explained in the paper. Simulation and practical test results for both IPMSM and RSM verify that accurate torque control can be achieved using this method. The practical implementation of the method is easy and should therefore be attractive for industrial drive applications.

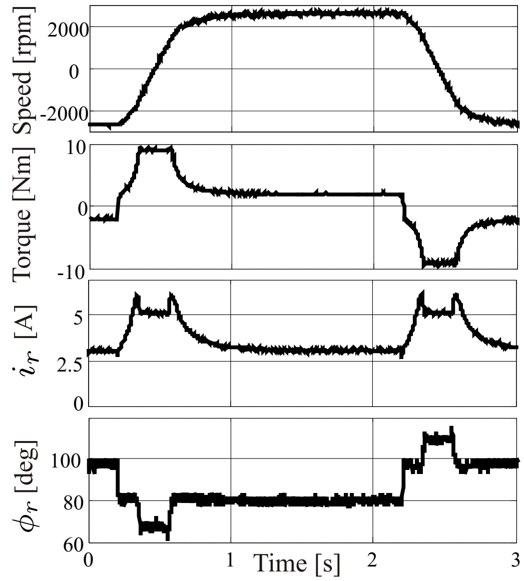

(a) RSM simulation dynamic test.

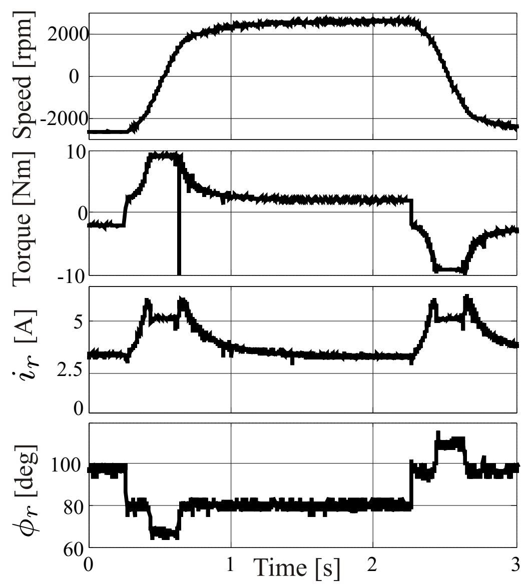

(b) RSM measured dynamic test.

Fig. 6. Practical and simulation results for RSM.

References

[1] H. de Kock, A. Rix, and M. Kamper, "Optimal torque control of interior permanent magnet synchronous machines in the full speed range," in *Proceedings of the 2008 International Conference on Electrical Machines (ICEM)*, 2008.

[2] H. de Kock, "Position sensorless and optimal torque control of reluctance and permanent magnet synchronous machines," Ph.D. dissertation, Stellenbosch University, South Africa, 2009.

[3] M. Kamper, M. Kamper, F. Van der Merwe, and S. Williamson, "Direct finite element design optimisation of the cageless reluctance synchronous machine," *Energy Conversion, IEEE Transaction on*, vol. 11, no. 3, pp. 547–555, 1996.

[4] A. Consoli, F. Russo, G. Scarcella, and A. Testa, "Low- and zero-speed sensorless control of synchronous reluctance motors," *Industry Applications, IEEE Transactions on*, vol. 35, no. 5, pp. 1050–1057, 1999.

[5] P. Guglielmi, M. Pastorelli, G. Pellegrino, and A. Vagati, "Position-sensorless control of permanent-magnet-assisted synchronous reluctance motor," *Industry Applications, IEEE Transactions on*, vol. 40, no. 2, pp. 615–622, 2004.

[6] N. Bianchi, S. Bolognani, J.-H. Jang, and S.-K. Sul, "Comparison of pm motor structures and sensorless control techniques for zero-speed rotor position detection," in *Power Electronics Specialists Conference, 2006. PESC '06. 37th IEEE*, 2006, pp. 1–7.

[7] A. Consoli, G. Scarcella, G. Scelba, A. Testa, and D. Triolo, "Sensorless rotor position estimation in synchronous reluctance motors exploiting a flux deviation approach," *Industry Applications, IEEE Transactions on*, vol. 43, no. 5, pp. 1266–1273, 2007.

[8] H. de Kock, M. Kamper, O. Ferreira, and R. Kennel, "Position sensorless control of the reluctance synchronous machine considering high frequency inductances," in *Power Electronics and Drive Systems, 2007. PEDS'07*, 2007.

[9] H. de Kock, M. Kamper, and R. Kennel, "Anisotropy comparison of reluctance and pm synchronous machines for low speed position sensorless applications," in *13th International Conference on Power*

Electronics and Motion Control (EPE-PEMC), 2008.

[10] N. Imai, S. Morimoto, M. Sanada, and Y. Takeda, “Influence of magnetic saturation on sensorless control for interior permanent-magnet synchronous motors with concentrated windings,” *Industry Applications, IEEE Transactions on*, vol. 42, no. 5, pp. 1193–1200, 2006.

[11] M. Rahman, L. Zhong, and K. W. Lim, “A direct torque-controlled interior permanent magnet synchronous motor drive incorporating field weakening,” *Industry Applications, IEEE Transactions on*, vol. 34, no. 6, pp. 1246–1253, 1998.

[12] H.-D. Lee, S.-J. Kang, and S.-K. Sul, “Efficiency-optimized direct torque control of synchronous reluctance motor using feedback linearization,” *Industrial Electronics, IEEE Transactions on*, vol. 46, no. 1, pp. 192–198, 1999.

[13] L. Zhong, M. Rahman, W. Hu, K. Lim, and M. Rahman, “A direct torque controller for permanent magnet synchronous motor drives,” *Energy Conversion, IEEE Transaction on*, vol. 14, no. 3, pp. 637–642, 1999.

[14] M. Haque, L. Zhong, and M. Rahman, “A sensorless initial rotor position estimation scheme for a direct torque controlled interior permanent magnet synchronous motor drive,” *Power Electronics, IEEE Transactions on*, vol. 18, no. 6, pp. 1376–1383, 2003.

[15] L. Tang, L. Zhong, M. Rahman, and Y. Hu, “A novel direct torque controlled interior permanent magnet synchronous machine drive with low ripple in flux and torque and fixed switching frequency,” *Power Electronics, IEEE Transactions on*, vol. 19, no. 2, pp. 346–354, 2004.

[16] M. Pacas and J. Weber, “Predictive direct torque control for the pm synchronous machine,” *Industrial Electronics, IEEE Transactions on*, vol. 52, no. 5, pp. 1350–1356, 2005.

[17] K. Gulez, A. Adam, and H. Pastaci, “A novel direct torque control algorithm for ipmsm with minimum harmonics and torque ripples,” *Mechatronics, IEEE/ASME Transactions on*, vol. 12, no. 2, pp. 223–227, 2007.

[18] Z. Xu and M. Rahman, “Direct torque and flux regulation of an ipm synchronous motor drive using variable structure control approach,” *Power Electronics, IEEE Transactions on*, vol. 22, no. 6, pp. 2487–2498, 2007.

[19] T. Geyer, G. Papafotiou, and M. Morari, “Model predictive direct torque control part i: Concept, algorithm, and analysis,” *Industrial Electronics, IEEE Transactions on*, vol. 56, no. 6, pp. 1894–1905, 2009.

[20] G. Papafotiou, J. Kley, K. Papadopoulos, P. Bohren, and M. Morari, “Model predictive direct torque control part ii: Implementation and experimental evaluation,” *Industrial Electronics, IEEE Transactions on*, vol. 56, no. 6, pp. 1906–1915, 2009.

[21] S. Morimoto, M. Sanada, and Y. Takeda, “Wide-speed operation of interior permanent magnet synchronous motors with high-performance current regulator,” *Industry Applications, IEEE Transactions on*, vol. 30, no. 4, pp. 920–926, 1994.

[22] S.-K. Chung, H.-S. Kim, C.-G. Kim, and M.-J. Youn, “A new instantaneous torque control of pm synchronous motor for high-performance direct-drive applications,” *Power Electronics, IEEE Transactions on*, vol. 13, no. 3, pp. 388–400, 1998.

[23] F.-J. Lin and R.-J. Wai, “A hybrid computed torque controller using fuzzy neural network for motor-quick-return servo mechanism,” *Mechatronics, IEEE/ASME Transactions on*, vol. 6, no. 1, pp. 75–89, 2001.

[24] R. Monajemy and R. Krishnan, “Control and dynamics of constant-power-loss-based operation of permanent-magnet synchronous motor drive system,” *Industrial Electronics, IEEE Transactions on*, vol. 48, no. 4, pp. 839–844, 2001.

[25] B.-H. Bae, N. Patel, S. Schulz, and S.-K. Sul, “New field weakening technique for high saliency interior permanent magnet motor,” in *Industry Applications Conference, 2003. 38th IAS Annual Meeting. Conference Record of the*, vol. 2, 2003, pp. 898–905 vol.2.

[26] C.-T. Pan and S.-M. Sue, “A linear maximum torque per ampere control for ipmsm drives over full-speed range,” *Energy Conversion, IEEE Transaction on*, vol. 20, no. 2, pp. 359–366, 2005.

[27] M. Bech, T. Frederiksen, and P. Sandholdt, “Accurate torque control of saturated interior permanent magnet synchronous motors in the field-weakening region,” in *Industry Applications Conference, 2005. Fourtieth IAS Annual Meeting. Conference Record of the 2005*, vol. 4, 2005, pp. 2526–2532 Vol. 4.

[28] Y.-R. Mohamed, “A newly designed instantaneous-torque control of direct-drive pmsm servo actuator with improved torque estimation and control characteristics,” *Industrial Electronics, IEEE Transactions on*, vol. 54, no. 5, pp. 2864–2873, 2007.

[29] R. Morales-Caporal and M. Pacas, “A predictive torque control for the synchronous reluctance machine taking into account the magnetic cross saturation,” *Industrial Electronics, IEEE Transactions on*, vol. 54, no. 2, pp. 1161–1167, 2007.

[30] A. Consoli, G. Scarcella, G. Scelba, S. Sindoni, and A. Testa, “Steady-state and transient analysis of maximum torque per ampere control for ipmsms,” in *Industry Applications Society Annual Meeting, 2008. IAS ’08. IEEE*, 2008, pp. 1–8.

[31] L. Serrano-Iribarnegaray and J. Martinez-Roman, “A unified approach to the very fast torque control methods for dc and ac machines,” *Industrial Electronics, IEEE Transactions on*, vol. 54, no. 4, pp. 2047–2056, 2007.

[32] F. Morel, J.-M. Retif, X. Lin-Shi, and C. Valentin, “Permanent magnet synchronous machine hybrid torque control,” *Industrial Electronics, IEEE Transactions on*, vol. 55, no. 2, pp. 501–511, 2008.

[33] A. J. Rix, M. J. Kamper, and R.-J. Wang, “Design and performance evaluation of concentrated coil permanent magnet machines for in-wheel drives,” in *Electric Machines & Drives Conference, 2007. IEMDC ’07. IEEE International*, M. J. Kamper, Ed., vol. 1, 2007, pp. 770–775.

[34] H. de Kock and M. Kamper, “Dynamic control of the permanent magnet-assisted reluctance synchronous machine,” *Electric Power Applications, IET*, vol. 1, no. 2, pp. 153–160, 2007.

Hugo W. de Kock (M’2006) received the M.Sc. (Eng.) and Ph.D. (Eng.) at Stellenbosch University, South Africa in 2006 and 2009 respectively. The focus of his Ph.D study was Position Sensorless and Optimal Torque control of Synchronous Machine Drives. He studied for two years at Wuppertal University, Germany as part of his Ph.D and was a DAAD scholarship holder. He is currently employed as a development engineer in the automotive industry and focuses on the application of electrical drives in electrical vehicles.

Arnold J. Rix (M’2007) received the B. (Eng) degree in 2004 at Stellenbosch University, South Africa. He is currently working towards his Ph.D. (Eng.) degree, focussing on in-wheel synchronous PM machines with concentrated windings for electrical vehicle applications. He is employed at Stellenbosch University where he presents an undergraduate practical course on electrical machines and drives.

Maarten J. Kamper (M’1995 - SM’2008) received the M.Sc. (Eng.) degree in 1987 and the Ph.D. (Eng.) degree in 1996 both from Stellenbosch University, South Africa. He has been with the academic staff of the Department of Electrical and Electronic Engineering, Stellenbosch University, since 1989, where he is currently a Professor of electrical machines and drives. His research interests include computer-aided design and control of reluctance, permanent magnet and induction machine drives. Prof. Kamper is a South African National Research Foundation Supported Scientist and a Registered Professional Engineer in South Africa.

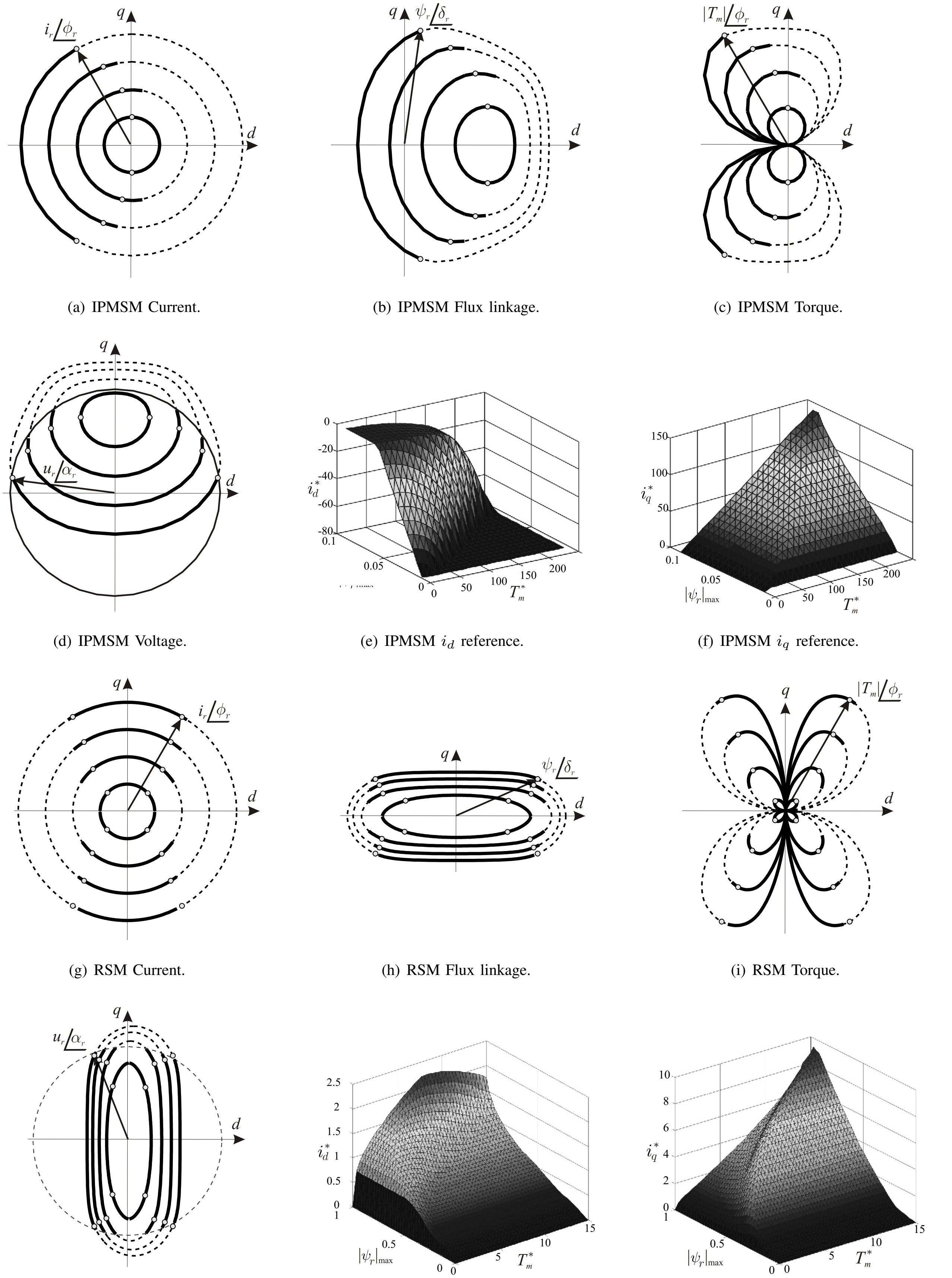

(a) IPMSM Current. (b) IPMSM Flux linkage. (c) IPMSM Torque.

(d) IPMSM Voltage. (e) IPMSM i_d reference. (f) IPMSM i_q reference.

(g) RSM Current. (h) RSM Flux linkage. (i) RSM Torque.

(j) RSM Voltage. (k) RSM i_d reference. (l) RSM i_q reference.

Fig. 2. FE results and torque control LUTs.